

Actin-Latrunculin A Structure and Function

DIFFERENTIAL MODULATION OF ACTIN-BINDING PROTEIN FUNCTION BY LATRUNCULIN A*

Received for publication, May 18, 2000, and in revised form, June 19, 2000
Published, JBC Papers in Press, June 19, 2000, DOI 10.1074/jbc.M004253200

Elena G. Yarmola, Thayumanasamy Somasundaram‡, Todd A. Boring, Ilan Spector§, and Michael R. Bubb¶||

From the Department of Medicine, University of Florida, Gainesville, Florida 32610, the ‡Institute of Molecular Biophysics, Florida State University, Tallahassee, Florida 32306, the §Department of Physiology and Biophysics, State University of New York, Stony Brook, New York 11794, and the ¶Research Service, Malcom Randall Department of Veterans Affairs Medical Center, Gainesville, Florida 32608

Latrunculin A is used extensively as an agent to sequester monomeric actin in living cells. We hypothesize that additional activities of latrunculin A may be important for its biological activity. Our data are consistent with the formation of a 1:1 stoichiometric complex with an equilibrium dissociation constant of 0.2 to 0.4 μM and provide no evidence that the actin-latrunculin A complex participates in the elongation of actin filaments. Profilin and latrunculin A bind independently to actin, whereas binding of thymosin β_4 to actin is inhibited by latrunculin A. Potential implications of this differential effect on actin-binding proteins are discussed. From a structural perspective, if latrunculin A binds to actin at a site that sterically influences binding by thymosin β_4 , then the observation that latrunculin A inhibits nucleotide exchange on actin implies an allosteric effect on the nucleotide binding cleft. Alternatively, if, as previously postulated, latrunculin A binds in the nucleotide cleft of actin, then its ability to inhibit binding by thymosin β_4 is a surprising result that suggests that significant allosteric changes affect the thymosin β_4 binding site. We show that latrunculin A and actin form a crystalline structure with orthorhombic space group $P2_12_12_1$ and diffraction to 3.10 Å. A high resolution structure with optimized crystallization conditions should provide insight regarding these remarkable allosteric properties.

Latrunculin A, isolated from the Red Sea sponge *Negombata magnifica*, was initially identified as an inhibitor of actin polymerization by its morphological effects and by the effects it had on actin filament distribution in cultured nonmuscle cells (1). Based on the effects of latrunculin A on the steady state level of F-actin *in vitro*, the effects of the drug were thought to be consistent with sequestration of monomeric actin in a 1:1 molar complex with equilibrium dissociation constant of 0.2 μM (2). The binding site of latrunculin has not been conclusively identified, but based on the study of the effects of specific mutations of yeast actin on latrunculin A binding, it has been inferred that latrunculin A may bind to actin near or in its nucleotide binding cleft (3, 4). The observation that latrunculin affects nucleotide exchange has been offered as support of this

conclusion (3). These data, however, are inconclusive in light of the fact that many actin-binding proteins with binding sites that are spatially distant from the nucleotide cleft are also able to affect nucleotide exchange (5) and that actin demonstrates several additional allosteric properties that serve as a precedent for the transmission of structural alterations to distant sites (6–8).

When latrunculin A is employed in studies of cell biology, the observed effects are consistent with depolymerization of actin filaments consequent to sequestration of monomeric actin by latrunculin (9). A previous preliminary report (2) did not rule out the possibility that latrunculin A has effects related to the polymerization of actin in addition to monomer sequestration, and these possibilities are explored in our current studies. Other effects of latrunculin A on the cytoskeleton are possible, however, and evidence has been reported that latrunculin can affect the expression of actin and possibly of other actin-binding proteins by a feedback mechanism that may sense the cellular concentration of actin monomers, resulting in more complicated outcomes than that predicted by monomer sequestration alone (10). To characterize the surface interactions of latrunculin A and actin, we examined whether latrunculin A affected the interaction of actin with other actin-monomer-binding proteins. To our surprise, latrunculin A inhibited binding by thymosin β_4 but not binding by profilin or DNase I. Because thymosin β_4 has been postulated to perform functions related to wound healing (11), apoptosis (12), and the inflammatory response (13), augmentation of the concentration of free thymosin β_4 by latrunculin A could potentiate these responses. Our results imply that actin-binding marine natural products may have effects other than those predicted solely by their effects on actin polymerization and, by inference, that marine natural products may exist that affect actin-binding protein function without directly affecting actin polymerization. Finally, our results illustrate a novel mechanism by which pharmacological agents that bind actin could be used to modulate the function of actin-binding proteins.

EXPERIMENTAL PROCEDURES

Materials—Rabbit skeletal muscle actin was prepared from frozen muscle (Pel-Freez, Rogers, AR) in Buffer G (5.0 mM Tris, 0.2 mM ATP, 0.2 mM dithiothreitol, 0.1 mM CaCl_2 , and 0.01% sodium azide, pH 7.8) (15), and pyrenyl-actin (actin labeled on Cys-374 with *N*-(1-pyrene)iodoacetamide) was prepared with 0.7–0.95 mol of label/mol of protein using the method of Kouyama and Mihashi (14). Recombinant human profilin was purified as described previously (15). Beef pancreatic DNase I (molecular biology grade; Worthington Biochemical Corp., Freehold, NJ) was reconstituted from lyophilized powder. Rat thymosin β_4 cDNA (which codes for an amino acid sequence identical to that of human thymosin β_4) in a pcDNA3 (Invitrogen, Carlsbad, CA) vector was a gift from Dr. Vivianne Nachmias (University of Pennsylvania

* The costs of publication of this article were defrayed in part by the payment of page charges. This article must therefore be hereby marked "advertisement" in accordance with 18 U.S.C. Section 1734 solely to indicate this fact.

|| Supported by the Medical Research Service of the Department of Veteran Affairs. To whom correspondence should be addressed: Box 100277, Dept. of Medicine, University of Florida, Gainesville, FL 32610. Tel.: 352-392-4059; Fax: 352-392-6481; E-mail: bubb@medicine.ufl.edu.

School of Medicine). Oligonucleotides were designed so as to add a cysteine residue to the C terminus, and both strands of the cloned products were sequenced to verify the outcome. After cloning into an pET-12a expression vector, the *Escherichia coli* strain BL21(DE3) was transformed with plasmid. Latrunculin A was stored as a 2 or 10 mM stock in Me₂SO and was diluted to 100 μM in Buffer G for the *in vitro* experiments.

Purification and Labeling of Thymosin β₄—Cells containing wild-type or cysteine-modified thymosin β₄ constructs were grown at 37 °C in M9 medium and harvested 3 h after induction with 1 mM isopropyl β-D-thiogalactopyranoside. Cell pellets were dissolved in 0.5 M cooled perchloric acid, sonicated for 2 min in ice, and centrifuged for 30 min at 4 °C (130,000 × g). The supernatant was adjusted to pH 7.0–7.5 with KOH and centrifuged to remove KClO₄. After the adjustment of pH to 4.0 with formic acid, the supernatant was rapidly heated to 80 °C for 10 min, chilled on ice for 10 min, centrifuged for 30 min at 4 °C, dialyzed against 20 mM formic acid, pH 4.0, and loaded on a SP-Hi Trap column (Amersham Pharmacia Biotech). The thymosin β₄ was eluted with a linear gradient of NaCl (0–2 M) in 20 mM formic acid, pH 4.0). The fractions were neutralized with 2M Tris base as soon as eluted and dialyzed against P buffer (5 mM Tris-HCl, 40 mM KCl, 0.2 mM dithiothreitol, 0.02% sodium azide, pH 7.9). Thymosin β₄ concentration was determined using the BCA protein assay (Bio-Rad).

For labeling, thymosin β₄ was dialyzed in 50 mM sodium borate buffer, and then tetramethylrhodamine-5-maleimide (T-6027, Molecular Probes Inc.) was added in four aliquots to a final molar ratio of dye to thymosin β₄ of 2:1. After 8 h of stirring at 33–34 °C, the sample was chilled on ice and left overnight. The reaction was stopped by addition of dithiothreitol, and the sample was dialyzed against P buffer. Thymosin β₄ was then gel-filtered with Superose-12 column, and the concentration of thymosin β₄ was determined by BCA protein concentration assay. Extent of labeling was determined using extinction coefficients for dye of ε₅₄₁ = 115 mM⁻¹ and ε₂₈₀ = 32.5 mM⁻¹. Modification of the C terminus with addition of an acetylated cysteine has previously been shown not to affect the actin binding properties of thymosin β₄ (16).

Steady State and Elongation Rate Measurements—Actin (4% pyrenyl-labeled) was converted to Mg²⁺-actin by the addition of 125 μM EGTA and 50 μM MgCl₂, and after 15 min, it was polymerized by the addition of MgCl₂ to a final concentration of 2.0 mM with varying KCl (or at 10 mM KCl and varying latrunculin A). Individual steady state samples were prepared by dilution of 10 μM F-actin without a change in buffer conditions, and steady state fluorescence readings were obtained at 24 h as described previously (17). Equilibrium dissociation constants were calculated assuming that the *x* intercepts reflected the total amount of unpolymerized actin, either as monomer or as a complex of latrunculin A and actin. The analysis assumes that fluorescence intensity is proportional to F-actin concentration. A seeded polymerization assay using gel-filtered cross-linked F-actin seeds was used to measure elongation rates of 4.0 μM Mg²⁺-actin as described previously (17). Preliminary data confirmed that the initial rate of polymerization was proportional to both the concentration of added seeds and to the concentration of free actin.

Nucleotide Exchange on Actin—Excess free ATP was removed using AG 1-X8 anion exchange resin (Bio-Rad) as described previously (18). Actin (1.7 μM) and profilin (0.2 μM) were incubated in a glass cuvette with Buffer G without ATP and various concentrations of latrunculin A. A mixture of εATP and KCl (final concentrations, 3.37 μM and 50 mM, respectively) was added to start the reaction. After mixing, samples were placed in spectrofluorometer, and the time course of fluorescence changes was recorded (15). Exchange rates were obtained by fitting the time course to a single exponential. Data were then fit to the following equilibrium dissociation constants: *K*_{actP}, for profilin to actin, *K*_{actL} for latrunculin A to actin, and *K*_{actLP} for profilin to the complex of actin and latrunculin A, and also to *k*_A, *k*_{AP}, *k*_{AL}, and *k*_{ALP}, the rate constants of ATP dissociation from actin, profilin, actin-latrunculin A, and actin-latrunculin A-profilin ternary complex, respectively.

Native Gel Electrophoresis—Actin at a concentration of 2.9 μM was incubated in Buffer G with or without 3.4 μM thymosin β₄ in the presence and absence of 40 μM latrunculin A. Solutions were incubated for 35 min before loading on gel. Native gels were equilibrated in buffer containing 0.1 mM CaCl₂, 0.01% sodium azide, 0.2 mM ATP, 0.2 mM dithiothreitol, and 25 mM Tris-Tricine, pH 8.2. In experiments with labeled thymosin β₄, the picture of the fluorescent gel was taken before staining with Coomassie.

Fluorescence Anisotropy—Data were collected on a Photon Technology International (South Brunswick, NJ) spectrofluorometer. Tetramethylrhodamine-5-maleimide-labeled thymosin β₄ was excited with vertically polarized light at 546 nm. The horizontal and vertical

components of the emitted light were detected at 568 nm. Solutions of labeled thymosin β₄ (0.1 μM) in Buffer G were titrated with Mg²⁺-actin in the presence or absence of a constant amount of latrunculin A (or with latrunculin A in the presence or absence of a constant amount of Mg²⁺-actin).

Data were fit globally as described by Vinson *et al.* (19), with the inclusion of a term for the formation of a ternary complex between actin, latrunculin, and thymosin. Fitting parameters included the equilibrium dissociation constants for thymosin β₄ to actin (*K*_{actT}), for latrunculin A to actin (*K*_{actL}), and for thymosin β₄ to the complex of actin and latrunculin A (*K*_{actLT}) and the terms indicating the anisotropy of free thymosin β₄ (*r*_f) and the anisotropy of the complex of thymosin β₄ with actin or with actin-latrunculin A complex (*r*_b). Assuming that the concentration of free thymosin, [T], is low relative to *K*_{actT}, (or strictly, [T]/*K*_{actT} ≪ (1 + [L]/*K*_{actL}), equations for the observed fluorescence anisotropy, *r*, can be written as a function of the total actin, [A]_t, and total latrunculin A, [L]_t, concentrations as follows,

$$r = r_f + (r_b - r_f) \left(1 - \frac{K_{actLT}}{[A]([L]_t/[A] + K_{actL}) + K_{actLT}/K_{actT} + K_{actLT}} \right) \quad (\text{Eq. 1})$$

$$[A] = \frac{((K_{actL} - [A]_t + [L]_t)^2 + 4[A]_t K_{actL})^{1/2} - (K_{actL} - [A]_t + [L]_t)}{2} \quad (\text{Eq. 2})$$

where [A] is free actin concentration.

Analytical Ultracentrifugation—Sedimentation equilibrium experiments were performed using absorption optics with data collected at 535 nm (the absorption maximum for labeled thymosin β₄) in a Beckman XLA centrifuge. All samples contained 1.6 μM labeled thymosin β₄. Samples of 110 μl in Buffer G reached equilibrium in 42 h at 13,900 rpm (after initially overspeeding to 15,100) at 4 °C. Buffer density was determined by pycnometry, and partial specific volumes were as previously reported for actin or calculated from amino acid sequence for thymosin β₄ (20). The gradient was analyzed according to a method of implicit constraints as described previously (21). In brief, at 535 nm, only labeled thymosin β₄ has a measurable extinction coefficient. The other sample components are invisible. Therefore, at this wavelength, the absorbance at any radius is directly proportional to the sum of the concentration of all allowable thymosin β₄-containing species (in a model of noncompetitive inhibition, these include thymosin β₄, thymosin β₄ bound to actin, and thymosin β₄-actin-latrunculin A ternary complex). The species are assumed to be in chemical equilibria at all radii as governed by appropriate equilibrium dissociation constants. Curve fitting is constrained by the initial concentration of all components, and the fitting parameters include only the dissociation constants and the concentration of each component at an arbitrary radius, *r*_b (21).

Measurement of DNase I Activity—DNase I (30 nM) was incubated with actin (30 nM) with varying concentrations of latrunculin A for 5 min at room temperature before adding 100 μg/ml DNA. The reaction mixture was in buffer containing 21 mM NaCl, 0.1 mM CaCl₂, 2.0 mM MgCl₂, 0.1 mM ATP, and 5 mM Tris, pH 7.9. After 20 min, samples were loaded on 0.7% agarose gels, and the gels were subsequently stained with ethidium bromide.

Crystallization of Latrunculin A and Actin—Crystals were grown in hanging droplets containing 1.3–1.5 M ammonium sulfate, 3 mM MgCl₂, 60 mM imidazole, pH 6.7, with actin concentration at 9 mg/ml and a ratio of 1:1 or 1.2:1 of latrunculin A to actin. Crystals appeared after 2–4 weeks at room temperature. Seemingly identical crystallization conditions produced satisfactory crystals only in approximately 50% of attempts. Crystals with typical dimensions 0.4 × 0.5 × 0.4 mm were wet mounted on glass capillaries at room temperature. The data were collected using Cu Kα radiation (λ = 1.541 Å) from a Rigaku RU-200 x-ray generator (40 kV, 90 mA, 0.3 mm collimator). The generator was equipped with an R-Axis IIC image plate, and data were collected at a crystal-IP distance of 100 mm with an oscillation range of 1.1 degree/frame. Data were integrated and scaled using the two companion programs of the HKL Suite, Denzo and Scalepack (22).

Crystal Density Measurements—Stock 50 or 60% Ficoll solutions in crystallization buffer, prepared according to Ref. 23, were mixed in the desired ratios with crystallization buffer to prepare solutions of various Ficoll concentrations. The density of each solution was calculated from the mass of 0.4 ml of solution as measured with a positive-displacement pipette. Ammonium sulfate was used to vary the buffer density for a given concentration of Ficoll. The technique relies on the assumption that ammonium sulfate, but not Ficoll, rapidly enters the solute component of the crystal. Crystals were layered on top of a step gradient of Ficoll in a 6-mm-diameter glass cuvette and immediately centrifuged at

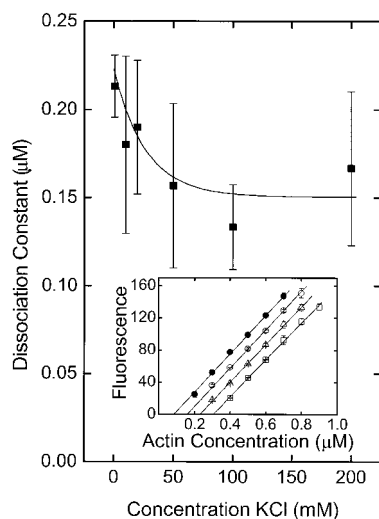


FIG. 1. Steady state determination of apparent critical concentration and equilibrium dissociation constant for latrunculin A as a function of salt concentration. The K_{dL} is calculated indirectly from the change in apparent critical concentration of 4% pyrenyl- Mg^{2+} -actin caused by $0.25 \mu M$ latrunculin A. Error bars represent ± 2 S.D. for measurements from three different actin preparations. The line through the data is arbitrary. *Inset*, steady state fluorescence data after 24 h in 10 mM KCl for 0 (filled circles), 0.25 (circles), 0.5 (triangles), and $0.75 \mu M$ (squares) latrunculin A. The lines through the data represent a least squares best fit. Error bars represent ± 2 S.D. for three samples made from the same F-actin stock.

$8000 \times g$ for 2 min. After the positions of crystals were located, the cuvette was centrifuged for an additional 1 min to check for changes in position. In control experiments, centrifugation time varied from 1 to 10 min. Some crystals were lightly cross-linked in 0.15% glutaraldehyde for 12 h at room temperature prior to density measurements. Whereas uncross-linked crystals were stable for only 10–15 min at low solvent density, the crystals were stable (with constant density) for several hours after covalent cross-linking. Crystal density as a function of the partial specific volume of the protomer was then calculated as described previously (23).

RESULTS

Steady State Fluorescence Data for F-actin Are Consistent with Formation of a 1:1 Complex of Latrunculin A and Actin with Little or No Dependence on Ionic Strength—The calculated concentration of latrunculin A-actin complex was proportional to the concentration of latrunculin A, consistent with monomer sequestration (Fig. 1, *inset*). The calculated equilibrium dissociation constant (K_{dL}) is similar to that previously reported ($K_{dL} = 0.2 \mu M$ in very low ionic strength buffer containing 0.1 mM $CaCl_2$ and 2.0 mM $MgCl_2$) (2). Latrunculin A did not cause any significant differences in the slopes of the curves for fluorescence *versus* actin concentration relative to controls, consistent with 1) the absence of actin-filament capping activity (24), and 2) similar binding affinity to pyrenyl-actin and unlabeled actin (25). The slight increase (or perhaps absence of change) in affinity at increasing ionic strength implies that electrostatic interactions contribute insignificantly to binding (Fig. 1).

The Initial Rate of Polymerization in a Seeded Polymerization Assay Fit a Model in Which the Latrunculin A-Actin Complex Did Not Participate in Elongation—Unlike the actin-monomer-binding protein, profilin, elongation data for actin in the presence of latrunculin A can be explained by monomer sequestration alone with K_{dL} of $0.22 \pm 0.06 \mu M$ (Fig. 2). Notably, although the data suggest that monomer sequestration is the most simple explanation for these data, they fail to prove that latrunculin A-actin complex does not participate in elongation, as any of a number of more complicated models are plausible in

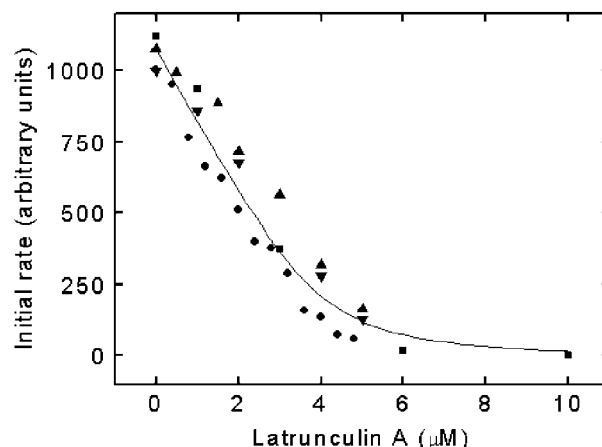


FIG. 2. Dependence of initial rates of seeded actin polymerization on latrunculin A concentration. Total actin concentration was $4 \mu M$. The squares, circles, upward-pointing triangles, and downward-pointing triangles represent four independent sets of data. The line represents the best simultaneous fit to all four sets of data assuming a critical concentration of $0.08 \mu M$ and a model of monomer sequestration by latrunculin A, in which case, K_{dL} is $0.22 \mu M$.

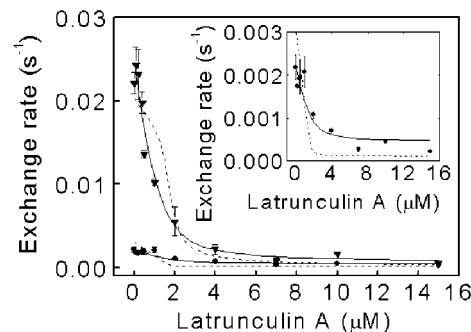


FIG. 3. Effects of profilin and latrunculin A on the rate of nucleotide exchange on actin. Rate of nucleotide exchange in the presence (triangles) and absence (circles) of $0.2 \mu M$ profilin is shown as a function of latrunculin A concentration. The *inset* shows the *bottom curve* with a magnified scale. The data are fit assuming that profilin and latrunculin A bind independently to actin (solid lines) or competitively to actin (dashed lines). Error bars represent \pm S.E. for three samples.

which the complex adds and dissociates in a nonproductive manner.

Profilin and Latrunculin A Bind Noncompetitively to Actin—Nucleotide exchange on actin was used to indirectly assess the interaction of latrunculin A with actin in the presence or absence of profilin (profilin, by itself, accelerates nucleotide exchange on actin (18)). Latrunculin A alone inhibited nucleotide exchange on $1.7 \mu M$ Mg^{2+} -actin, as previously reported (Fig. 3, *inset*) (3). Latrunculin A also inhibited nucleotide exchange in the presence of profilin (Fig. 3), implying either that latrunculin A bound competitively with profilin to actin or that nucleotide exchange on actin was inhibited in the ternary complex of latrunculin A, profilin, and actin. Quantitative evaluation of the data eliminated the possibility that binding was competitive. Consistent with fluorescence anisotropy data (data not shown), profilin binds to actin with equilibrium dissociation constant, K_{dP} , of $0.1 \mu M$ under these experimental conditions. Assuming this K_{dP} and a model of competitive binding, the data could not be fit by any possible combination of binding constants of latrunculin A to actin and exchange rates for the complexes of profilin-actin and latrunculin A-actin (Fig. 3, *dashed line*). Also, the best possible fit required an unreasonable K_{dL} for latrunculin A-actin ($0.009 \mu M$) when compared

TABLE I
Equilibrium dissociation constants organized by experimental technique

Equilibrium dissociation constants are listed for binding latrunculin A to actin (K_{dL}), thymosin β_4 to actin (K_{dT}), thymosin β_4 to actin saturated with latrunculin A (K_{dLT}), and profilin to actin (K_{dP}). Data used for calculation of each constant are shown in the figures indicated. Error estimates are based on a standard least squares deviation fitting algorithm with 95% confidence limits.

Type of experiment	K_{dL}	K_{dT}	K_{dLT}	K_{dP}^a
		μM		
Steady state (Fig. 1)	0.15–0.22			
Seeded polymerization (Fig. 2)	0.22 ± 0.06			
Nucleotide exchange (Fig. 3)	0.28 ± 0.28			0.1
Fluorescence anisotropy (Fig. 5)	0.35 ± 0.05	0.23 ± 0.02	7.65 ± 0.74	
Seeded polymerization (Fig. 5)	0.40 ± 0.05	0.31 ± 0.03		
Analytical ultracentrifugation (Fig. 5)	0.52 ± 0.18	0.92 ± 0.28	8.0 ± 1.9	

^a K_{dP} defined from fluorescence anisotropy experiments (data not shown).

with the other results reported here. In contrast, a model in which profilin and latrunculin A bound independently to actin provided a good fit to the experimental data and yielded a reasonable K_{dL} for latrunculin A-actin ($0.28 \mu\text{M}$; in Table I, the large error estimate for K_{dL} in the nucleotide exchange experiment relative to the other experimental methods reported here is due to the large number of fitting parameters). Moreover, the best possible global fit to the data was achieved when latrunculin A and profilin were allowed to interact cooperatively with actin, so that the affinity of latrunculin A for actin was increased by a factor of 1.8 when profilin was bound. The fit achieved by allowing this minor degree of positive cooperativity (Hill coefficient of 1.1) was not significantly improved in comparison to a more simple, independent binding model. We conclude that the data rule out competitive binding, but the presence of either slight positive cooperativity or no cooperativity can plausibly explain the experimental results.

For the nucleotide exchange experiments, profilin concentration was constant ($0.2 \mu\text{M}$) and not saturating; therefore, the exchange rate with no latrunculin A (0.023 s^{-1}) is not equal to k_{AP} ; rather, k_{AP} was obtained as the best global fit to the data. Assuming noncompetitive binding, the best global fit for the exchange rate constants was obtained with $k_{AP} = 0.137 \text{ s}^{-1}$, $k_A = 0.0015 \text{ s}^{-1}$, $k_{AL} = 0.0003 \text{ s}^{-1}$, and $k_{ALP} = 0.0011 \text{ s}^{-1}$. Values for k_A and k_{AP} are consistent with previous reports (26). The fit curves are insensitive to relatively large changes in k_{AL} and k_{ALP} , and these parameters cannot be distinguished from 0 by the given data.

Native Gel Electrophoresis Provides Qualitative Evidence That Latrunculin A Inhibits Binding of Thymosin β_4 to Actin—The addition of latrunculin A to samples containing mixtures of thymosin β_4 and actin caused less actin to shift to a band corresponding to a high electrophoretic mobility complex of thymosin β_4 and actin, implying that the complex is dissociated by latrunculin A (Fig. 4, compare lanes 3 and 4). Similarly, less fluorescently labeled thymosin β_4 shifted to the band corresponding to this complex in the presence of latrunculin A (Fig. 4, compare lanes 1 and 2). Previous results have suggested that the extent of binding seen in this assay may not quantitatively reflect the apparent K_d for thymosin β_4 and actin (27), perhaps because of excluded volume effects, but changes in the amount of shifted protein are qualitatively indicative of the extent of formation of a thymosin β_4 -actin complex. The data also show that unlabeled thymosin β_4 bound as well to actin as labeled thymosin β_4 and that binding to actin was inhibited by latrunculin A to the same extent as covalently labeled thymosin β_4 (Fig. 4, lanes 7–10).

Experiments Providing Quantitative Data Show That Latrunculin A Decreases the Affinity of Thymosin β_4 for Actin by Approximately 1 Order of Magnitude—Fluorescence anisotropy of labeled thymosin β_4 increased from 0.08 when free to 0.18 when saturated with actin. The anisotropy was lower in the

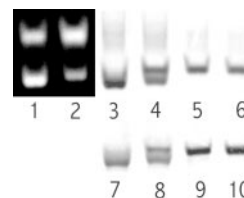


FIG. 4. **Qualitative assessment of competition between thymosin β_4 and latrunculin A for actin using a native gel.** Actin ($2.9 \mu\text{M}$) was incubated with (lanes 1–4, 7, and 8) or without (lanes 5, 6, 9, and 10) thymosin β_4 ($3.4 \mu\text{M}$) and run on a nondenaturing electrophoretic gel. In lane 1, fluorescently labeled thymosin β_4 separates into two bands. The low mobility band at the top is free thymosin β_4 , and the high mobility band is thymosin β_4 that is bound to actin. In lane 2, $40 \mu\text{M}$ latrunculin A is also present, and much less thymosin β_4 is bound to actin. The identical gel samples are shown in lanes 3 and 4 after Coomassie staining, in which actin is the primary protein visualized. In lane 3, actin is shifted to the same position as actin-bound thymosin β_4 . Latrunculin A causes less actin to shift (lane 4). Samples of actin alone and actin with latrunculin A are shown as unshifted controls in lanes 5 and 6, respectively. The samples in lanes 7–10 are identical to those in lanes 3–6 except that the thymosin β_4 is unlabeled.

presence of latrunculin A than in its absence at any given actin concentration, indicating that latrunculin A inhibits binding of thymosin β_4 to actin (Fig. 5A, top panel). Increasing latrunculin A at fixed actin concentration caused dissociation of thymosin β_4 from actin (Fig. 5A, bottom panel); if binding was independent (that is, if K_{dT} is equal to the equilibrium dissociation constant for binding of thymosin β_4 to latrunculin A-actin complex, K_{dLT}), then these curves would be flat. In contrast, the best global fit to all four data sets was obtained with $K_{dT} = 0.23 \pm 0.02 \mu\text{M}$, $K_{dL} = 0.35 \pm 0.05 \mu\text{M}$, and $K_{dLT} = 7.65 \pm 0.74 \mu\text{M}$. Therefore, this assay implies inhibition by latrunculin A, with approximately 33 times (the ratio of K_{dLT} to K_{dT}) weaker affinity of thymosin β_4 for actin when latrunculin A is bound to actin.

Measurement of the elongation rate after seeding actin polymerization provides additional information regarding the interaction of latrunculin A, thymosin β_4 , and actin (Fig. 5B). The data obtained for equivalent amounts of latrunculin A and thymosin β_4 were nearly indistinguishable, therefore implying that the effects of thymosin β_4 on filament elongation, like those of latrunculin A, can be explained by a simple model of monomer sequestration and that the binding constants K_{dL} and K_{dT} are similar. The observation that latrunculin A and thymosin β_4 have an additive effect on actin polymerization rates is demonstrated graphically in Fig. 5B, consistent with competitive binding by the two ligands on actin. If binding of the ligands occurred independently, then the effect of a mixture of components would be less than the effect of either component alone at a concentration equal to the sum of the components. Quantitative analysis of the elongation data confirms that a competitive binding model, but not an independent binding

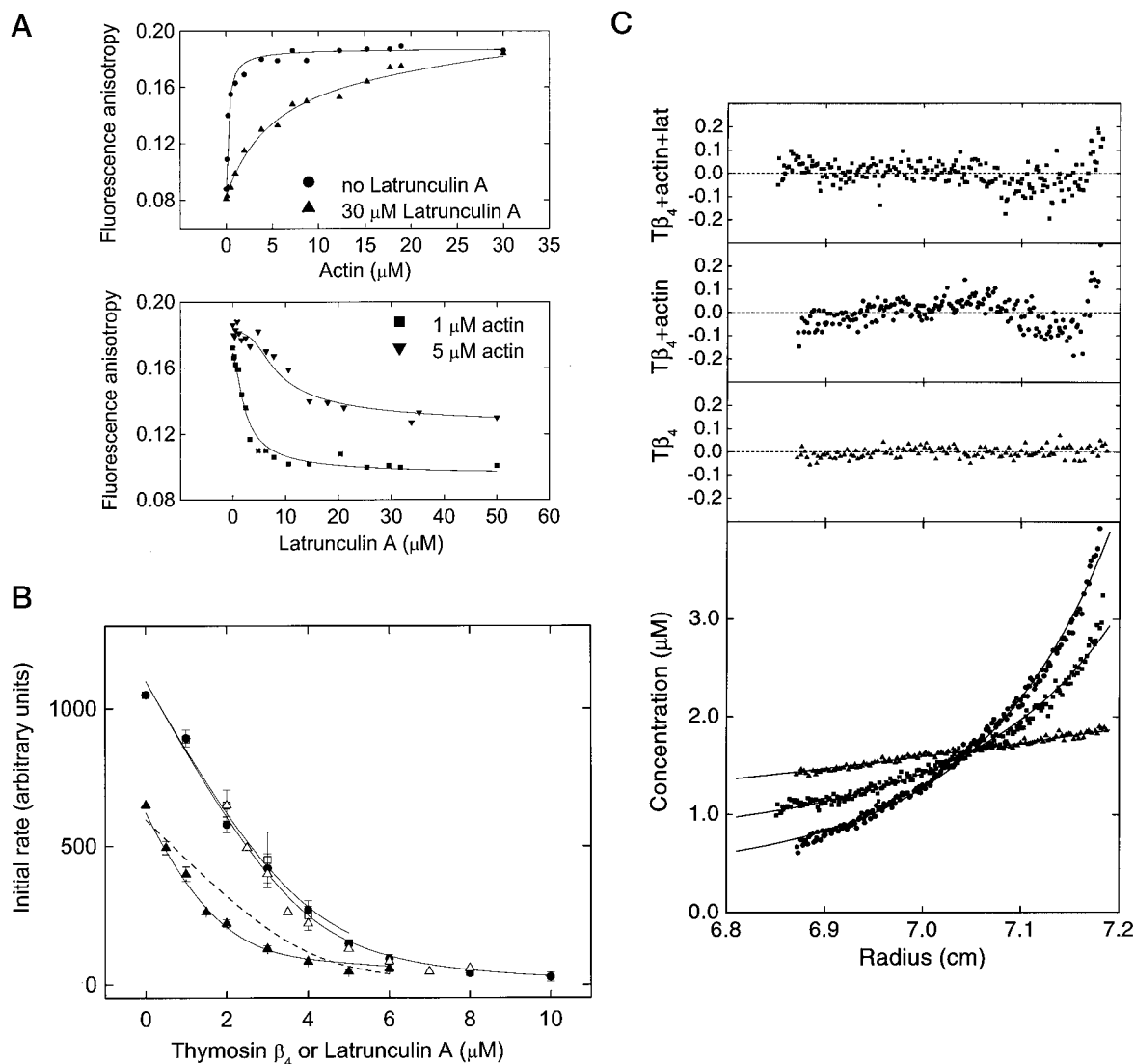


FIG. 5. Quantitative assays of competition between thymosin β_4 and latrunculin A for actin. *A*, fluorescence anisotropy showing titration of 0.1 μM solutions of labeled thymosin β_4 with actin in presence (triangles) and absence (circles) of 30 μM latrunculin A (top panel) and titration of 0.1 μM solutions of labeled thymosin β_4 with latrunculin A in presence of 1 μM (squares) and 5 μM (triangles) actin (bottom panel). The solid lines show the result of a global fit to the data, with $K_{dT} = 0.23 \mu\text{M}$, $K_{dL} = 0.35 \mu\text{M}$, and $K_{dLT} = 7.65 \mu\text{M}$. *B*, the initial rate of seeded actin polymerization is shown as a function of the concentration of latrunculin A (open squares), thymosin β_4 (filled circles), or in the presence of a fixed concentration of latrunculin A (2.0 μM) as a function of the concentration of thymosin β_4 (filled triangles). Total actin concentration was 4 μM . Solid lines represent the best simultaneous fit to all three sets of data assuming competitive binding, with $K_{dL} = 0.40 \mu\text{M}$ and $K_{dT} = 0.31 \mu\text{M}$. The dashed line shows the best fit assuming independent binding, with $K_{dL} = 0.30 \mu\text{M}$ and $K_{dT} = 0.26 \mu\text{M}$. The same data obtained at fixed latrunculin A concentration and various concentrations of thymosin β_4 are replotted as a function of the concentration of latrunculin A and thymosin β_4 (open triangles) to illustrate that the mixture of the two ligands yields essentially indistinguishable results from those obtained if either component was replaced with the other. This would be predicted if thymosin β_4 and latrunculin A bind to actin with similar K_d and if binding is competitive, but not if binding was independent. *C*, sedimentation equilibrium gradients for 1.6 μM labeled thymosin β_4 (triangles), 1.6 μM labeled thymosin β_4 and 3.0 μM actin (circles), and 1.6 μM labeled thymosin β_4 , 3.0 μM actin, and 8.0 μM latrunculin A (squares). Only the labeled thymosin β_4 is visible at the recorded wavelength, and the absorbance at any radius is therefore directly proportional to the concentration of thymosin β_4 . The different gradients reflect different apparent molecular weights of thymosin β_4 resulting from complex formation with the other ligands. The shallower gradient observed after addition of latrunculin A reflects inhibition of binding between actin and thymosin β_4 , resulting in less actin bound to thymosin β_4 and therefore a lower average apparent molecular weight. The solid lines show the result of a global fit to the data assuming molecular weights consistent with atomic formulae and a noncompetitive model of inhibition, with $K_{dT} = 0.92 \mu\text{M}$, $K_{dL} = 0.52 \mu\text{M}$, and $K_{dLT} = 8.0 \mu\text{M}$. The differences between the actual data and the theoretical fit are shown in the three top panels.

model, adequately explains all the data for both ligands. The best global fit to the data, assuming competitive binding with a critical concentration of 0.08 μM , yields $K_{dL} = 0.40 \pm 0.05 \mu\text{M}$, $K_{dT} = 0.31 \pm 0.03 \mu\text{M}$. Although these data do not require a more complicated model that includes a finite K_{dLT} to generate a good fit, the results are insufficiently sensitive to distinguish between noncompetitive inhibition (finite K_{dLT}) and a more simple competitive binding model (infinite K_{dLT}).

Sedimentation equilibrium experiments also graphically illustrate inhibition of the thymosin β_4 ligand by latrunculin A

(Fig. 5C). Samples were made with 1.6 μM labeled thymosin β_4 with or without 3.0 μM actin and either 8.0 μM latrunculin A or an equivalent volume of Me_2SO . Use of labeled thymosin β_4 allows for large and easily detectable changes in the apparent molecular weight of thymosin β_4 upon binding to the much larger molecule, actin. The observation of a steeper exponential gradient in a sample of thymosin β_4 with actin than for thymosin β_4 alone is therefore due to the formation of an actin-thymosin β_4 complex (Fig. 5C, compare circles and triangles). If binding of the thymosin β_4 and latrunculin A ligands on actin

occurs independently, then the data with or without latrunculin A would be indistinguishable (Fig. 5C, compare *circles* and *squares*). Rather, binding of thymosin β_4 to actin was inhibited by latrunculin A, with the following best estimates for equilibrium dissociation constants: $K_{dL} = 0.52 \pm 0.18 \mu\text{M}$, $K_{dT} = 0.92 \pm 0.28 \mu\text{M}$, and $K_{dLT} = 8.0 \pm 1.9 \mu\text{M}$. The data for thymosin β_4 alone demonstrate a slight extent of systematic deviation from the theoretical curve, consistent with a small amount of dimeric protein (3% dimer according to an analysis not shown). Although native thymosin β_4 has been reported to be monomeric (28), this small extent of dimerization may have previously escaped detection or be a unique result related to bacterial expression of protein or covalent labeling. Perhaps dimerization of thymosin β_4 explains the systematic deviation observed in the plots for the data that includes actin, with a small amount of dimeric thymosin β_4 binding to two actin molecules (only visible at large radius and high actin concentrations).

The results of all quantitative assays for latrunculin A-actin interactions are shown in Table I. The variation of reported equilibrium dissociation constants in Table I probably reflects limitations of the techniques and true differences related to differences between binding to Ca^{2+} -actin and Mg^{2+} -actin and difference in ionic strength, but it is also possible that they reflect true pressure-related changes that occur during analytical centrifugation.

Latrunculin A Did Not Inhibit the Binding of DNase I to Actin—The endonuclease activity of DNase I is inhibited by actin. Measurement of the activity of DNase I by assay of DNA fragmentation has previously been used to show that the actin-binding protein gelsolin can displace actin from DNase I (29). Using the same assay, we were unable to detect any increase in the activity of DNase I in the presence of saturating concentrations (up to $20 \mu\text{M}$) of latrunculin A (data not shown). A control using DNase I with or without latrunculin A ruled out the possibility that latrunculin A was by itself an inhibitor of DNase I. The high affinity interaction between actin and DNase I (K_a of approximately 10^{10}M^{-1} (29)) limits the detection of small changes in affinity between DNase I and actin. A 6-fold drop in affinity with the given experimental conditions (30 nM DNase I and 30 nM actin) would be predicted to increase the amount of free DNase I from 1.7 to 4.0 nM. Control experiments determined that the assay conditions could reliably detect a change of this magnitude. Therefore, we conclude that latrunculin A does not inhibit DNase I-actin interactions, or if it does so, the inhibition is minimal.

Inhibition of Polymerization by Latrunculin A Results in the Formation of a Unique Actin Crystal—Crystals were shown to contain both latrunculin A and actin by mass spectroscopy and gel electrophoresis, respectively. X-ray diffraction resulted in a data set that was 99.9% complete for the range 40.0–3.2 Å with an overall $R_{\text{merge}} (\sum_h \sum_i I_{h,i} \cdot \langle I_h \rangle / \sum_h \sum_i I_{h,i})$ of 11.2%, and for the highest resolution shell, 3.44–3.34 Å, the R_{merge} was 32.2%, with an average $I/\sigma I = 3.5$ (Fig. 6, A and B). The crystal belongs to the orthorhombic space group $P2_12_12_1$ with unit cell dimensions of $a = 101.68$, $b = 103.09$, and $c = 127.12$ Å; $\alpha = \beta = \gamma = 90.0^\circ$. Systematic absences were consistent with the space group assignment of $P2_12_12_1$ (for $h00$, $h \neq 2n$; for $0k0$, $k \neq 2n$; and for $00l$, $l \neq 2n$). At least 12 systematically absent reflections were measured for each of the three axes. Detailed summaries of the data collection statistics are shown in Table II. The crystals diffracted to 3.10 Å or better at 300 K; however, a complete data set could be processed only up to 3.2 Å using two crystals. All crystals examined ($n = 5$), however, resulted in data consistent with orthorhombic space group $P2_12_12_1$ and similar unit cell dimensions. Crystal density was consistent

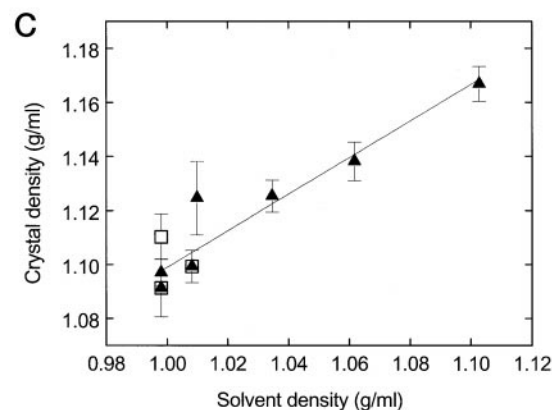
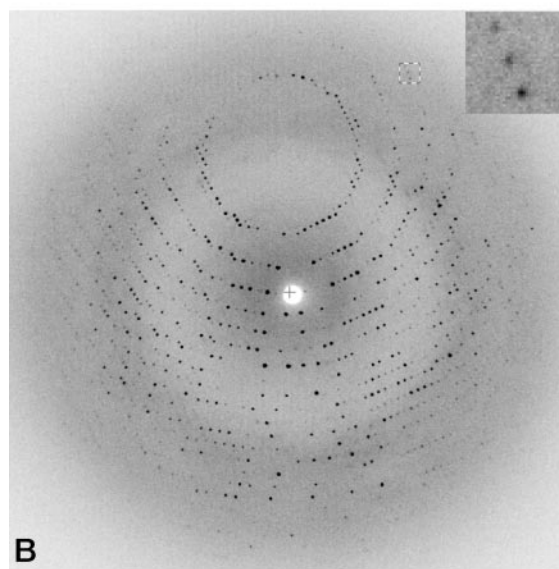
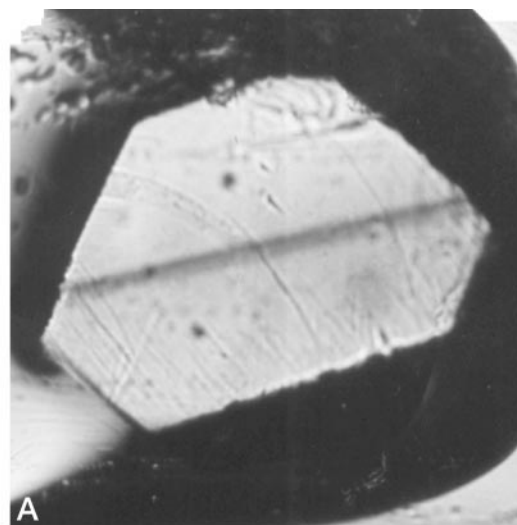


FIG. 6. Crystals of actin and latrunculin A. A, photograph of actin-latrunculin A crystal measuring 0.75 mm in its longest dimension. B, diffraction pattern obtained from pictured crystal. The highest resolution seen is approximately 3.10 Å (*inset*). C, results of crystal density measurements in step gradients of Ficoll using either intact crystals (*solid triangles*) or crystals cross-linked with glutaraldehyde (*open squares*). Each *data point* represents the result for a single crystal, and the *error bars* define the upper and lower limits of the step in the gradient at which the crystal reached equilibrium. Variation along the *x* axis is achieved by varying the sample concentration of ammonium sulfate. The best fit with n set to 8 (or two protomers per asymmetric unit) gives a partial specific volume of $\bar{v} = 0.765 \text{ ml/g}$ (*solid line*).

TABLE II
Data collection statistics for crystals of latrunculin A and actin

Data gathered	Value
Crystal density	1.098 mg/ml in water
Resolution limits (Å)	40.0–3.34
Space group	P2 ₁ 2 ₁ 2 ₁
Unit cell dimensions (Å)	$a = 101.68$, $b = 103.09$, $c = 127.12$ Å; $\alpha = \beta = \gamma = 90.0^\circ$
Number of total observations	132,524
Number of unique observations	26,342
Completeness (%)	99.9
R_{merge} (%)	32.2
Protomers per asymmetric unit	2
Protein volume fraction	28%

with eight molecular complexes per unit cell (Fig. 6C). Calculation of the Matthews coefficient for a crystal with assumed actin:latrunculin A stoichiometry of 1:1 resulted in the V_M value of 3.94 Å³/dalton with 72% solvent content if two protomers are assumed to be in the asymmetric unit (30). These values are within the range observed for other proteins. We are currently calculating the self-rotation function to ascertain the observed symmetry and to look for any other noncrystallographic symmetry elements.

DISCUSSION

Our current data show that in the presence of latrunculin A, profilin binds to actin independently, or perhaps with some positive cooperativity. Similarly, latrunculin A had no apparent effect on actin-DNase I interactions. In contrast, binding of thymosin β_4 to actin is inhibited by latrunculin A. Previous reported information suggested that latrunculin A bound to actin in the cleft between subdomains 2 and 4 of actin, at a site adjacent to the adenine nucleotide binding site (3). We confirm that latrunculin A inhibits adenine nucleotide exchange on actin. Just as DNase I, which bridges the cleft between subdomains 2 and 4, reduces the rate of adenine nucleotide exchange on actin (31), latrunculin A may limit the flexibility of the cleft and trap nucleotide, thereby resulting in relative inhibition of nucleotide exchange.

Inhibition of the binding of thymosin β_4 to actin by latrunculin A does not necessarily conflict with the postulated localization of latrunculin A to the nucleotide-binding cleft of actin. Neither the analytical ultracentrifuge data nor the fluorescence anisotropy data are consistent with simple competitive inhibition (in which case, $(K_{DLT})^{-1} = 0$), but rather, they suggest that latrunculin A inhibits thymosin β_4 noncompetitively. Noncompetitive inhibition of thymosin β_4 binding to actin by latrunculin A has several possible structural interpretations. Latrunculin A could bind near or at the binding site of thymosin β_4 , but not be large enough to create a steric effect that completely eliminates simultaneous binding by thymosin β_4 . Because evidence has been reported that thymosin β_4 may bind to actin in an extended conformation, with interactions on actin at multiple sites (5), a second possibility is that latrunculin A sterically competes at one site of interaction, and the weak affinity of thymosin β_4 in the presence of latrunculin A is due to residual interactions between actin and thymosin β_4 at other sites. The third possibility is that latrunculin A inhibits binding by an allosteric effect, perhaps with a binding site in the nucleotide binding cleft of actin, as previously suggested.

The most recent models of thymosin β_4 bound to actin show that thymosin β_4 is more than 20 Å from the nucleotide binding cleft (5, 8). In these analyses, earlier evidence that thymosin β_4 could be covalently cross-linked to ATP γ S (32) was considered to be an artifact produced by cross-linking free, rather than actin-bound, nucleotide to thymosin β_4 . Although considerable evidence supports the identification of an interaction between

subdomain 1 of actin and thymosin β_4 (5, 32, 33), disagreement continues regarding whether thymosin β_4 binds directly to subdomain 2 of actin (5) or whether the effects on subdomain 2 can be explained by an allosteric mechanism (33). To summarize, if latrunculin A does bind in the nucleotide-binding cleft of actin, then effects on thymosin β_4 are the result of substantial allosteric effects on actin. Conversely, latrunculin A may bind at or near one of the thymosin β_4 binding sites on actin and, like thymosin β_4 , allosterically affect the rate of nucleotide exchange.

Proteins that bind to actin may regulate actin filament dynamics and may have functions independent of their actin-regulatory functions. Moreover, these functions may be regulated by their interaction with actin filaments or monomers. Profilin and thymosin β_4 have proven to be typical examples for which identification of actin-regulatory functions has been followed by the identification of complex functions that may, in turn, be dependent on actin binding activity. The regulation of phosphoinositide metabolism by profilin and the roles of thymosin β_4 in wound healing, apoptosis, and immunosuppression illustrate the diversity of functions served by such proteins (12, 13, 11, 34). With latrunculin A, we have demonstrated that a drug that binds to actin may have differential effects on various actin-binding proteins. Given the independent functions of these actin-binding proteins, the effects of actin-binding drugs may have far-reaching consequences. First, these effects may be significant when the drugs are employed to dissect cell biological problems. Thus, the consequences of addition of latrunculin A to cells *in vivo* or *in situ* may be the result of factors other than simple monomer sequestration. Secondly, our preliminary work with more than 20 derivatives of latrunculin A suggests that derivatization may independently alter properties of monomer sequestration and inhibition of thymosin β_4 binding. Finally, it may be possible to exploit these effects in a therapeutic context.

With regard to the effects of thymosin β_4 on immune suppression, thymosin β_4 sulfoxide appears to be an effector molecule for the anti-inflammatory effect of glucocorticoids (13). It is not known how thymosin β_4 gets sulfonated or gets to the extracellular space, but it is certainly possible that only free thymosin β_4 actively participates in either one or both of these steps. If so, latrunculin A may activate the anti-inflammatory function of thymosin β_4 by increasing free thymosin β_4 concentrations. Thus, actin-binding drugs may induce specific, desired effects by a novel mechanism. Because several cell regulatory proteins, such as protein kinases and their substrates, are spatially regulated by anchorage to F-actin (35–37), the potential displacement and activation of these proteins by actin-binding drugs suggests that this general mechanism may, in other instances, have broad implications with complicated consequences.

Latrunculin A lowers the affinity of actin for thymosin β_4 by approximately 1 order of magnitude. Although this is not a large thermodynamic effect, it is likely to be significant in living cells. In a cell such as a polymorphonuclear leukocyte with approximately 150 μM thymosin β_4 (38), the addition of saturating concentrations of latrunculin A would result in a rapid change in the effective equilibrium dissociation constant for thymosin β_4 from approximately 0.3 (K_{DT}) to 8 μM (K_{DLT}). Assuming that the critical concentration of actin in a cell is maintained at approximately 1.0 μM by capping of barbed ends, this would be expected to cause an immediate increase in the amount of free thymosin β_4 by approximately 15 μM . If excluded volume conditions in the cytoplasm increase the relative affinity of these interactions by a factor of 10, which is a conservative estimate (39), then the concentration of free thy-

mosin β_4 would increase 3-fold immediately after adding latrunculin A. Later, as actin depolymerizes and the complex of actin-latrunculin A begins to accumulate, this complex becomes a sink for monomer sequestering proteins, particularly those that bind to the complex as well as they bind to free actin. Thus, at steady state, both free profilin and free thymosin β_4 concentrations would be diminished after addition of latrunculin A, but because of the differential effect of latrunculin A, the decrease in profilin concentration would be much greater than that for thymosin β_4 .

The actin crystal described here is unique because it is the first actin crystal to diffract to this resolution in the absence of other actin-binding proteins. It is also unique in its symmetry and packing volume. The successful use of a marine natural product inhibitor of actin polymerization to stabilize actin for purposes of crystallization may have other applications. In cases in which production of an actin crystal in complex with other proteins or peptides of interest has been unsuccessful to date, the addition of latrunculin A or another actin-stabilizing marine natural product may facilitate crystal growth.

REFERENCES

1. Spector, I., Shochet, N. R., Kashman, Y., and Groweiss, A. (1983) *Science* **214**, 493–495
2. Coué, M., Brenner, S. L., Spector, I., and Korn, E. D. (1987) *FEBS Lett.* **213**, 316–318
3. Ayscough, K. R., Stryker, J., Pokala, N., Sanders, M., Crews, P., and Drubin, D. G. (1997) *J. Cell Biol.* **137**, 399–416
4. Belmont, L. D., Patterson, G. M. L., and Drubin, D. G. (1999) *J. Cell Sci.* **112**, 1325–1336
5. Safer, D., Sosnick, T. R., and Elzinga, M. (1997) *Biochemistry* **36**, 5806–5816
6. Kuznetsova, I., Antropova, O., Turoverov, K., and Khaitlina, S. (1996) *FEBS Lett.* **383**, 105–108
7. Prochniewicz, E., and Thomas, D. D. (1997) *Biochemistry* **36**, 12845–12853
8. De La Cruz, E. M., Ostap, E. M., Brundage, R. A., Reddy, K. S., Sweeney, H. L., and Safer, D. (2000) *Biophys. J.* **78**, 2516–2527
9. Spector, I., Shocet, N. R., Blasberger, D., and Kashman, Y. (1989) *Cell Motil. Cytoskeleton* **13**, 127–144
10. Bershadsky, A. D., Gluck, U., Denisenko, O. N., Sklyarova, T. V., Spector, I., and Ben-Zéev, A. (1995) *J. Cell Sci.* **108**, 1183–1193
11. Frohm, M., Gunne, H., Bergman, A. C., Agerberth, B., Bergman, T., Boman, A., Liden, S., Jörnvall, H., and Boman, H. G. (1996) *Eur. J. Biochem.* **237**, 86–9
12. Niu, M., and Nachmias, V. T. (2000) *Cell Adhes. Commun.* **7**, 311–320
13. Young, J. D., Lawrence, A. J., MacLean, A. G., Leung, B. P., McInnes, I. B., Canas, B., Pappin, D. J. C., and Stevenson, R. D. (1999) *Nat. Med.* **5**, 1424–1427
14. Kouyama, T., and Mihashi, K. (1981) *Eur. J. Biochem.* **114**, 33–38
15. Kang, F., Laine, R. O., Bubb, M. R., Southwick, F. S., and Purich, D. L. (1997) *Biochemistry* **36**, 8384–8392
16. Carlier, M.-F., Didry, D., Erk, I., Lepault, J., Van Troys, M. L., Vanderkerckhove, J., Perelroizen, I., Yin, H., Doi, Y., and Pantaloni, D. (1996) *J. Biol. Chem.* **271**, 9231–9239
17. Bubb, M., Spector, I., Beyer, B. B., and Fosen, K. M. (2000) *J. Biol. Chem.* **275**, 5163–5170
18. Mockrin, S. C., and Korn, E. D. (1980) *Biochemistry* **19**, 5359–5362
19. Vinson, V. K., De La Cruz, E. M., Higgs, H. N., and Pollard, T. D. (1998) *Biochemistry* **37**, 10871–10880
20. Kirschner, M. W., and Schachman, H. K. (1971) *Biochemistry* **10**, 1900–1925
21. Bubb, M. R., Lewis, M. S., and Korn, E. D. (1991) *J. Biol. Chem.* **266**, 3820–3826
22. Otwinowski, Z., and Minor, W. (1997) *Methods Enzymol.* **276**, 307–326
23. Westbrook, E. M. (1985) *Methods Enzymol.* **114**, 187–196
24. Terry, D. R., Spector, I., Higa, T., and Bubb, M. R., (1997) *J. Biol. Chem.* **272**, 7841–7845
25. Lal, A. A., and Korn, E. D. (1985) *J. Biol. Chem.* **260**, 10132–10138
26. Selden, L. A., Kinoshita, H. J., Estes, J. E., and Gershman, L. C. (1999) *Biochemistry* **38**, 2769–2778
27. Safer, D., Golla, R., and Nachmias, V. T. (1990) *Biochemistry* **87**, 2536–2540
28. Yu, F., Lin, S., Morrison-Bogorad, M., Atkinson, M. A. L., and Yin, H. L. (1993) *J. Biol. Chem.* **268**, 502–509
29. Davoodian, K., Ritchings, B. W., Ramphal, R., and Bubb, M. R. (1997) *Biochemistry* **36**, 9637–9641
30. B. W. Matthews (1968) *J. Mol. Biol.* **33**, 491–497
31. Polzar, B., Nowak, E., Goody, R. S., and Mannherz, H. G. (1989) *Eur. J. Biochem.* **182**, 267–275
32. Reichert, A., Heintz, D., Echner, H., Voelter, W., and Faulstich, H. (1996) *J. Biol. Chem.* **271**, 1301–1308
33. Ballweber, E., Hannappel, E., Huff, T., and Mannherz, H. G. (1997) *Biochem. J.* **327**, 787–793
34. Huff, T., Ballweber, E., Humeny, A., Bonk, T., Becker, C., Müller, C. S. G., Mannherz, H. G., and Hannappel, E. (1999) *FEBS Lett.* **464**, 14–20
35. Freeman, J. L., De La Cruz, E. M., Pollard, T. D., Lefkowitz, R. J., and Pitcher, J. A. (1998) *J. Biol. Chem.* **273**, 20653–20657
36. Prekeris, R., Hernandez, R. M., Mayhew, M. W., White, M. K., and Terrian, D. M. (1998) *J. Biol. Chem.* **273**, 26790–26798
37. Bubb, M. R., Lenox, R. H., and Edison, A. S., (1999) *J. Biol. Chem.* **274**, 36472–36478
38. Cassimeris, L., Safer, D., Nachmias, V. T., and Zigmund, S. H. (1992) *J. Cell Biol.* **119**, 1261–1270
39. Minton, A. P. (2000) *Curr. Opin. Struct. Biol.* **10**, 34–39